Fast Particle Finite Orbit Width and Larmor Radius Effects on Low-n Toroidicity induced Alfvén Eigenmode Excitation

N. N. Gorelenkov *, C. Z. Cheng, G. Y. Fu

Princeton Plasma Physics Laboratory, P.O. Box 451

Princeton, NJ 08543-0451

(January 13, 1999)

The effects of finite drift orbit width (FOW) and finite Larmor radius (FLR) of fast particles on the stability of low-n toroidicity-induced Alfvén eigenmodes (TAE) are studied. The formulation is based on the solution of the low frequency gyro-kinetic equation ($\omega \ll \omega_c$, where ω_c is particle cyclotron frequency) by following the particle drift orbit and thus fully retains the FOW effect. A quadratic form has been derived in terms of invariant variables: energy $\mathcal{E}$, magnetic moment μ, and toroidal angular momentum P_φ. The growth rate of TAE is computed perturbatively by numerically averaging over the fast particle drift orbit. These new computational capabilities improve the previous version of NOVA-K code [Fu G. Y., Cheng C. Z., Wong K. L., *Phys. Fluids B* **5** 4040 (1994)] which includes FOW effects in the growth rate calculation based on a small radial orbit width approximation. The new NOVA-K version has been benchmarked for different regimes of TAE excitation. It is shown that both FOW and FLR effects are typically stabilizing: the TAE growth rate can be reduced by as much as a factor of 2 for the Tokamak Fusion Test Reactor supershots [D. J. Grove and D. M. Meade, Nucl. Fusion **25**, 1167 (1985)]. However, FOW may be destabilizing for global TAEs, which usually have considerable amplitude in the outer radius region.

*Permanent address: TRINITI, Troitsk, Moscow region, 142092 Russia

[0]PACS numbers:52.35.Hr,52.35.Py,52.55.Pi

I. INTRODUCTION

Toroidicity-induced Alfvén Eigenmodes (TAE) have been studied for more than a decade since their theoretical prediction [1,2]. TAEs are of major importance to tokamak fusion reactors due to the possibility of ejecting alpha particles and other fast ions from the plasma core, possibly leading to degraded ignition margin and localized heat load on plasma facing components. Both experimental [3,4] and theoretical [5] studies demonstrate the possibility of fast particle transport induced by TAE.

TAEs can be excited via resonant interaction with fast particles when particle parallel velocity equals to Alfvén velocity v_A. Fast particles with density profile peaked at the plasma center can expand radially releasing their energy due to the TAE instability. In present day tokamaks, the drift orbits of fast particles, such as particles produced by the neutral beam injection (NBI), ion cyclotron resonance heating (ICRH) etc., have finite radial orbit width (FOW) and finite Larmor radius (FLR) comparable to the TAE mode scale length. A large radial displacement of particle orbit may reduce the fast particle drive because fast particles can interact with the mode only on the part of their trajectory which intersects the mode localization region. On the other hand, it is also possible that the FOW effects can enhance the TAE drive by allowing fast particles from the plasma center, where their density is high, to reach global modes with appreciable amplitude in the outer radius region. Thus, it is important to understand those effects through numerical simulations in order to make the code applicable for interpretation of the experimental data.

When first reported, the NOVA-K code include neither FOW nor FLR effects, [6] making use of the assumption that particles are moving in the magnetic surfaces. FOW effects were incorporated later in the NOVA-K [7] based on a linear radial expansion of particle drift orbit around the average particle drift flux surface. Such an approximation is valid only if the orbit width Δ_b is less than the magnetic surface minor radius. Moreover, the fast ion finite Larmor radius (FLR) effects are also important in determining the TAE stability. One notes that FLR are important when $k_\perp \rho_h \simeq nq\rho_h/r \sim 1$, where $k_\perp$ is mode perpendicular wavevector, ρ_h is fast particle Larmor radius, and q is the safety factor. If we assume that $r/\rho_h \simeq 10$, then FLR become important for modes with $n \geq 10/q$ at the mode localization. Provided the safety factor is within $1-5$ one can see that low-n TAEs may be affected by alpha particle FLR.

Here, we present an improved formulation of the NOVA-K code that includes both full FOW and FLR effects for calculating the TAE growth rate perturbatively. Numerical results from the improved NOVA-K code will be compared with the previous results.

Our derivation of the quadratic form, which will be used to calculate the mode growth rate, is performed for general axisymmetric tokamak equilibria. It is based on the solution of the low mode frequency gyro-kinetic equation with $\omega \ll \omega_c$, where ω_c is the particle cyclotron frequency. A quadratic form has been derived in terms of invariant variables: the particle energy $\mathcal{E}$, the magnetic moment μ, and the toroidal angular momentum P_φ. The growth rate of TAE is computed perturbatively by averaging over the full fast particle drift orbit. Our formulation is similar to that of Ref. [8], which utilizes guiding center particle Lagrangian and does not include the FLR effects. In addition, our formulation is designed for improving the NOVA-K code: it is represented in terms of NOVA coordinate variables and it has an explicit poloidal harmonic dependence.

The paper is organized as follows. In Section II we present the formulation of the quadratic form and the perturbative technique. Results of benchmarking the improved version of NOVA-K code with previous codes as well as the results of full FOW and FLR effects on the TAE stability are given in Section III. The summary is presented in Section IV.

II. FORMULATION

A. Particle Drift Orbit

We describe particle guiding center orbit in terms of adiabatic constants of motion:

$$\mathcal{E} = v^2/2$$

$$\mu = \mathcal{E}_\perp/B$$

$$P_\varphi = z\psi(R,Z)/Mc - \sigma_{||}\sqrt{2\mathcal{E}}\sqrt{1-\mu B/\mathcal{E}}(RB_\varphi/B), \tag{1}$$

where z and M are the charge and the mass of a particle, $(R,\ \varphi,\ Z)$ are the cylindrical coordinate with R being the major radius, φ the toroidal angle and Z along the tori symmetry axis, $\mathbf{b} = \mathbf{B}/B$, $\mathbf{B}$ is the equilibrium magnetic field, ψ is the poloidal magnetic flux, and $\sigma_{||}$ is the sign of particle parallel velocity, which equals 1 for particle parallel velocity directed in the same direction as the plasma current and equals -1 otherwise. In Fig. 1 we illustrate the particle orbits in the (R,ψ) space and the same orbits represented in the (R,Z) space as indicated by arrows. Fig. 1(a) shows a passing particle orbit and Fig. 1(b) shows a trapped particle orbit for an equilibrium, which corresponds to DT shot # 103101 at 2.92s in the Tokamak Fusion Test Reactor (TFTR) experiments [10], where TAE mode activity was observed [11]. The correspondiong plasma parameters are taken from the TRANSP analyzing code [12] and will be given in Section III. In our approach the drift orbit is represented by the $P_\varphi = const$ curve. The segments of the $P_\varphi = const$ curve above the $\psi(R,Z=0)$ (the poloidal flux in the midplane) curve in the (R,ψ) space corresponds to the particle guiding center orbit inside the plasma. Passing and trapped particle orbits may be obtained by looking for the intersection of particle orbit defined by $z\psi(R,Z)/Mc = P_\varphi + \sigma_{||}\sqrt{2\mathcal{E}}\sqrt{1-\mu B/\mathcal{E}}(RB_\varphi/B)$ and $\psi(R,Z=0)$ (see Ref. [9] for details).

The particle guiding center velocity is governed by [13]:

$$\frac{d\mathbf{r}_c}{dt} = v_{||}\mathbf{b} + \omega_c^{-1}\left(v_{||}^2\mathbf{b}\times\kappa + \mu\mathbf{b}\times\nabla B\right) =$$
$$= v_{||}\left[\mathbf{b} - \frac{v_{||}}{\omega_c}(\mathbf{b}\nabla\times\mathbf{b})\mathbf{b}\right] + \frac{v_{||}}{\omega_c}\nabla\times v_{||}\mathbf{b}, \tag{2}$$

where κ is the magnetic field curvature, $\mathbf{r}_c = \mathbf{r} + \mathbf{v}\times\mathbf{b}/\omega_c$ is the guiding-center, $\mathbf{r}$ is the particle position, and $\mathbf{v}$ is the particle velocity. The particle parallel velocity $v_{||}$ is a function of space coordinates. We present the axisymmetric equilibrium magnetic field in a general form:

$$\mathbf{B} = RB_\varphi \nabla\varphi + \nabla\varphi \times \nabla\psi, \tag{3}$$

where B_φ is the toroidal magnetic field. Using Eqs.(1)-(3) one obtains the following form for the particle guiding center velocity:

$$\frac{d\mathbf{r}_c}{dt} = \frac{v_\|}{\omega_c RB_\varphi}\mathbf{B} \times \nabla P_\varphi + \frac{v_\| B}{RB_\varphi}\frac{\nabla\varphi}{|\nabla\varphi|^2}. \tag{4}$$

The guiding center velocity in the form of Eq.(4) differs from that given in Ref. [9] as it includes all components of particle drift motion in a tokamak rather than only its toroidal projection.

B. Gyrokinetic Equation

To derive the fast particle response to low-n MHD perturbations, such as TAE modes, and to include FLR effects we will make use of the solution of the gyrokinetic equation given in Ref. [14]. We will adopt the arguments of Bessel functions in the form $v_\perp \nabla_\perp/\omega_c$, which operates on the perturbed quantities. This is justified for most practical cases with TAE toroidal mode numbers $n \geq 2$, when $r > \nabla_\perp^{-1}$. Thus, the perturbed distribution function for fast ions can be expressed in the form:

$$\begin{aligned} f = g + \frac{\mathbf{A}\times\mathbf{b}}{B}\nabla F + \frac{z}{M}\left[\phi F'_{\mathcal{E}} + \left(\phi - \frac{v_\|}{c}A_\|\right)\frac{F'_\mu}{B}\right] \\ - \frac{z}{MB}F'_\mu\left[J_0\left(\phi_c - \frac{v_\|}{c}A_{\|c}\right) + \frac{M\mu}{z}\left(J_0 + J_2\right)B_{\|c}\right], \end{aligned} \tag{5}$$

where subscript "c" means that the corresponding value is taken at the particle gyro-center $\mathbf{r}_c$, F is the equilibrium particle distribution function, $F'_x \equiv \partial F/\partial x$, ϕ and $\mathbf{A}$ are the electrostatic and the vector potentials, respectively, and J_l is the l-th order Bessel function. In this paper we will use the traditional representation of the perturbed quantities:

$$\begin{aligned} A(\mathbf{r},t) = e^{-i\omega t}\sum_m A_m(\psi)e^{iS_m}, \\ S_m = m\theta - n\varphi, \end{aligned} \tag{6}$$

where θ is the poloidal angle. The nonadiabatic part of the perturbed distribution function, $g = g(\mathbf{r}_c, t)$, satisfies the following equation:

$$\frac{dg}{dt} \equiv \left(\frac{\partial}{\partial t} + v_{\|}\mathbf{b}\nabla + \mathbf{v}_d\nabla\right) g$$
$$= \frac{z}{M}\left(i\omega F'_{\mathcal{E}} - \omega_c^{-1}\nabla F\mathbf{b}\times\nabla\right)\left[J_0\left(\phi_c - \frac{v_{\|}}{c}A_{\|c}\right) + \frac{M\mu}{z}\left(J_0 + J_2\right)B_{\|c}\right], \tag{7}$$

where $\mathbf{v}_d = d\mathbf{r}_c/dt - v_{\|}\mathbf{b}$ is the particle drift velocity. Energetic particles are not effected by the parallel electric field, which, therefore, is assumed to be zero and is realted to the vector potential by $E_{\|} = -\nabla_{\|}\phi - c^{-1}\partial A_{\|}/\partial t = 0$. This implies

$$\frac{\partial\phi}{\partial t} + \frac{v_{\|}}{c}i\omega A_{\|} = \frac{d\phi}{dt} - v_d\nabla\phi. \tag{8}$$

One can redefine the nonadiabatic part of the distribution function as follows:

$$\bar{g} = g - \frac{iz}{M\omega}\left(i\omega F'_{\mathcal{E}} - \omega_c^{-1}\nabla F\mathbf{b}\times\nabla\right)J_0\phi_c, \tag{9}$$

which now satisfies the equation:

$$\frac{d\bar{g}}{dt} = \frac{z}{M}\left(F'_{\mathcal{E}} + \frac{i\mathbf{b}\times\nabla}{\omega_c\omega}\nabla F\right)\left[J_0\mathbf{v}_d\nabla\phi_c + \frac{i\omega M\mu}{z}\left(J_0 + J_2\right)B_{\|c}\right]. \tag{10}$$

In the drift approximation, the particle equilibrium distribution function is a function of integrals of motion defined in Eq.(1)), which leads to:

$$F'_{\mathcal{E}} + \frac{i\nabla F}{\omega\omega_c}\mathbf{b}\times\nabla = F'_{\mathcal{E}} + \frac{iF'_{P_\varphi}}{\omega}\frac{\nabla\varphi\nabla}{|\nabla\varphi|^2} - \frac{iRB_\varphi}{v_{\|}B\omega}F'_{P_\varphi}\frac{d}{dt}, \tag{11}$$

where $d/dt = -i\omega + (d\mathbf{r}_c/dt)\cdot\nabla$ is used. Thus, we can make use of Eqs.(5,9) and rewrite the perturbed distribution function in the following form:

$$f = \hat{g} + \frac{z}{M}\left[F'_{\mathcal{E}} + \frac{F'_\mu}{B}\left(1 + \frac{i}{\omega}v_{\|}\nabla_{\|}\right) + \frac{i}{B\omega}F'_{P_\varphi}\nabla_{\|}\right](\phi - J_0\phi_c)$$
$$- \frac{\mu}{B}F'_\mu\left(J_0 + J_2\right)B_{\|c} - \frac{\nabla P_\varphi\times\mathbf{b}}{B}\mathbf{A}F'_{P_\varphi} - \frac{iz}{BM\omega}F'_{P_\varphi}\nabla\psi\times\mathbf{b}J_0\nabla\phi_c, \tag{12}$$

where now the nonadiabatic part is redefined as $\hat{g}$ which satisfies

$$\frac{d}{dt}\hat{g} = \frac{z}{M}\frac{\partial F}{\partial\mathcal{E}}\left(\omega - \omega_*\right)\hat{X}. \tag{13}$$

Here we have introduced the following notations:

$$\omega_* = -i \frac{\partial F/\partial P_\varphi}{\partial F/\partial \mathcal{E}} \frac{\partial}{\partial \varphi},$$
$$\hat{X} = \left(\frac{d\mathbf{r}_c}{dt} - v_{\|}\mathbf{b} \right) J_0 \nabla \phi_c + \frac{i\mu\omega M}{z} F'_\mu \left(J_0 + J_2 \right) B_{\|c}. \quad (14)$$

The expression for $\hat{X}$ can be simplified if we assume the perturbed electric field to be $\mathbf{E}_\perp = -\nabla_\perp \phi$ by neglecting the contribution from the vector potential $\mathbf{A}_\perp$. This approximation is valid because the $\mathbf{A}_\perp$ term is smaller than the $B_{\|c}$ term in Eq.(14) by a factor of $O(\epsilon/nq) \ll 1$. Thus we can write [6]:

$$\hat{X} \simeq \frac{i\omega M}{q} \left[(2\mathcal{E} - 3\mu B) J_0 \kappa \xi_\perp - \mu B J_0 \nabla \xi_\perp \right], \quad (15)$$

where the following ideal MHD description was adopted:

$$\mathbf{E} = \frac{i\omega}{c} \xi \times \mathbf{B}$$
$$\tilde{\mathbf{B}} = \nabla \times \mathbf{A} = \nabla \times (\xi \times \mathbf{B}), \quad (16)$$

with $\tilde{\mathbf{B}}$ being the perturbed magnetic field.

C. Perturbation Theory

The perturbation theory is based on a quadratic form, which can be obtained from the linearized momentum equation

$$\omega^2 \rho \xi = \nabla \tilde{p}_c + \nabla \tilde{\pi} + (4\pi)^{-1} (\tilde{\mathbf{B}} \times \nabla \times \mathbf{B} + \mathbf{B} \times \nabla \times \tilde{\mathbf{B}}), \quad (17)$$

where $\tilde{p}_c$ is the perturbed core plasma pressure, $\tilde{\pi} = \int \mathbf{v}\mathbf{v} f d\mathbf{v}$ is fast particle pressure tensor, ξ is the plasma displacement, and ρ is the plasma mass density. Considering the fast particle contribution as a small perturbation, one can obtain a quadratic form from Eq.(17) [6], and determine the TAE growth rate due to fast particle resonant interaction with the waves:

$$\gamma_h/\omega \simeq \Im(\delta W_k / 2\delta K), \quad (18)$$

where $\delta K = \omega^2 \int \rho|\xi|^2 d\mathbf{r}$ is the inertial energy. The imaginary part of the hot particle contribution to the potential energy is determined by the nonadiabatic part of the distribution function

$$\delta W_k = \int \xi^* \cdot \nabla \tilde{\pi} d\mathbf{r} = -\int\int \hat{g}\mathbf{v} \cdot (\mathbf{v} \cdot \nabla)\xi^* d\mathbf{r} d\mathbf{v}. \tag{19}$$

The plasma displacement at $\mathbf{r}$ is defined through the one at $\mathbf{r}_c$ as $\xi(\mathbf{r}) = e^{\hat{L}}\xi_{\mathbf{c}}(\mathbf{r}_c)$, where $\hat{L}$ should be treated as an operator: $\hat{L} = (\mathbf{b} \times \mathbf{v}_\perp/\omega_c) \cdot \nabla$. It is convenient to perform integration in Eq.(19) in the guiding center coordinates:

$$\delta W_k = -\int\int \hat{g} e^{\hat{L}^*} \mathbf{v} \cdot (\mathbf{v} \cdot \nabla)\xi_c^* d\mathbf{r}_c d\mathbf{v}. \tag{20}$$

Performing the gyro phase average [14] the fast particle contribution to the potential energy is reduced to the form

$$\delta W_k = \frac{-iq}{\omega} \int \hat{X}^* g d\mathbf{r}_c d\mathbf{v}. \tag{21}$$

Next, we make use of the coordinate system of particle integrals of motion Eqs.(1). One can show straightforwardly that the phase space integration is transformed as follows [8,15]

$$d\mathbf{r}_c d\mathbf{v} = (2\pi)^2 \sum_{\sigma_\parallel} \frac{B}{\omega_c} dP_\varphi d\mu d\mathcal{E} \frac{d\psi}{|\mathbf{v}_d \cdot \nabla\psi|} = (2\pi)^2 \sum_{\sigma_\parallel} \frac{B}{\omega_c} dP_\varphi d\mu d\mathcal{E} dt, \tag{22}$$

where we have used Eq.(4). Here dt is associated with fast drift motion, and the sum is over the signs of the particle parallel velocity.

D. Solution of Nonadiabatic Particle Distribution Function

The solution of the gyrokinetic equation Eq.(13) is given by

$$g = \frac{q}{M} \int^t F'_{\mathcal{E}} (\omega - \omega_*) \hat{X} dt', \tag{23}$$

where the time integration is to be taken along the unperurbed particle drift trajectory. We introduce the "drift" frequency as $\omega_{Dm} \equiv dS_m/dt$ (see Eq.(6)) and assume $S_m(t = 0) = 0$ for the simplicity, which allows us to write

$$\hat{X} = \sum_{ml} e^{-i\omega t + i\bar{\omega}_{Dm} t} X_{ml} e^{il\omega_b t}, \; X_{ml} = \tau_b^{-1} \oint dt' \hat{X}_m e^{i\int^{t'} (\omega_{Dm} - \bar{\omega}_{Dm} - l\omega_b) dt''}, \tag{24}$$

where ω_b is the frequency of particle periodic motion (with period τ_b) in plasma toroidal cross section, known as trapped particle bounce frequency or passing particle transit frequency, and $\bar{\omega}_{Dm}$ is the orbit averaged drift frequency. Then, Eq.(23) becomes

$$g = \frac{iq}{M} \sum_{ml} \frac{F'_{\mathcal{E}} \left(1 - \omega_*/\omega\right) X_{ml}}{\omega - \bar{\omega}_{Dm} - l\omega_b} e^{-it(\omega - \bar{\omega}_{Dm} - l\omega_b)}. \tag{25}$$

Substituting this expression into Eq.(19) we obtain

$$\delta W_k = -\frac{(2\pi M)^2 c\omega}{z} \int dP_\varphi d\mu d\mathcal{E} dt \sum_{mm'll'} \mathcal{E}^2 \frac{G^*_{m'l'} F'_{\mathcal{E}} \left(1 - \omega_*/\omega\right) G_{ml}}{\omega - \bar{\omega}_{Dm} - l\omega_b} e^{-it(\bar{\omega}_{Dm'} - \bar{\omega}_{Dm} + (l-l')\omega_b)}, \tag{26}$$

where $G_{ml} = -izX_{ml}/\omega M\mathcal{E}$ is defined the same way as in Ref. [6].

Defining "trapped" particles as those with drift trajectories not encircling the magnetic axis one can easily show that for this group of particles

$$\bar{\omega}_{Dm} = \bar{\omega}_{Dm}\big|_{m=0} \equiv \bar{\omega}_{D0}. \tag{27}$$

Then, using Landau prescription for the integration in energy we obtain from Eq.(26) the trapped particle contribution

$$\Im\delta W_k = i\frac{(2M)^2 \pi^3 c\omega}{z} \int dP_\varphi d\mu \sum_{mm'l} G^*_{m'l} G_{ml} \frac{\mathcal{E}^{5/2} \tau_b \sqrt{2} F'_{\mathcal{E}} \left(1 - \omega_*/\omega\right)}{\left|(\bar{\omega}_{D0} + l\omega_b)'_v\right|}, \tag{28}$$

where $G_{ml} = \tau_b^{-1} \oint dt' \hat{G}_m e^{i\int^{t'} (\omega_{Dm} - \omega) dt''}$, and the integrand should be taken at the resonance velocity determined by the resonance condition $\omega - \bar{\omega}_{D0} - l\omega_b = 0$. Defining "passing" particles as those encircling the magnetic axis, we transform the resonance condition using $\bar{\omega}_{Dm} = m\omega_b\sigma_{||} + \bar{\omega}_{D0}$. With the substitution $\tilde{l} = m\sigma_{||} + l$ we again obtain Eq.(28) for the passing particle contribution. Note that an equivalent formula, but without FLR effects, was obtained in Ref. [8]. Also, Eq.(28) has an explicit poloidal harmonic dependence, which allows it to be straightforwardly incorporated into the NOVA-K code.

III. RESULTS

A. Zero Orbit Width Limit

We benchmark the results of the new version of the NOVA-K code developed here for full orbit width (see Eqs.(18,28)) against the previous version reported in Ref. [7], which used small orbit width approximation. We begin with the zero orbit width limit, which is achieved by using an artificially large particle charge $z_h \to \infty$. The tokamak Plasma is chosen to have circular magnetic surfaces and the following parameters are used: $R_0 = 10m$ and $a = 0.9m$ are major and minor radii of the last magnetic surface, respectively, $B_0 = 3T$, $q(r = 0) = 1.6$, $q_a = q(r = a) = 2.2$. The safety factor profile is chosen to be a parabolic and only a single Alfvén gap is formed in the plasma for the toroidal mode number $n = 2$. The eigenmode in this case is represented well by two poloidal harmonics with $m = 3, 4$, which are highly localized at the $q = 1.75$ magnetic surface. The eigenfrequency is $\omega = 0.616\omega_A$, where $\omega_A = v_{A0}/q_a R_0$, and $v_{A0} = 6.54 \times 10^8 cm/s$ is the central Alfvén velocity. The plasma density profile is taken to be constant for simplicity with $n_i = n_e = 0.5 \times 10^{14} cm^{-3}$. The plasma core ions are assumed to be deuterium. The hot particle species is chosen to have a Maxwellian distribution function with a proton mass and a large charge $z_h = 10^6$. Thus there is effectively no hot particle destabilizing contribution from the pressure gradient and only hot particle Landau damping due to velocity space gradient remains. The result of comparison is presented in Fig 2. Shown also is the result using the following analytical formula for the Landau damping of Maxwellian ions:

$$\frac{\gamma_d}{\omega} = \frac{q^2\sqrt{\pi}\beta}{(\omega^2 4q^2/q_a^2\omega_A^2)}(F(x_r) + F(x_r/3))$$
$$F(x) = x^2\left(\frac{1}{2} + x^2 + x^4\right)e^{-x^2};\ x_r = \frac{2q\omega v_{A0}}{q_a\omega_A v_{Th}}, \tag{29}$$

where the thermal velocity is $v_{Th} = \sqrt{2T_h/m_h}$. This analytic formula is applicable here because the aspect ratio is large and the eigenmode is very localized. Good agreement is obtained for both codes within $\leq 1\%$ as we scan the hot particle temperature, which changes the ratio v_{Th}/v_A.

B. FOW and FLR Effects in Model Equilibrium

To study the effects of FOW and FLR we will use the equilibrium as presented in the Section III A, but with more realistic aspect ratio, i.e. we choose major radius $R_0 = 3m$. The thermal velocity of hot particles is fixed at $v_{Th} = v_A$. The particle charge is artificially varied in the range $z_h = 0.25 - 100$ so that the radial orbit width changes from a small orbit width to one that is comparable to the eigenmode radial width. This way, we can study a smooth transition from zero orbit width to large orbit width limit. The TAE eigenmode structure, shown in Fig. 3, is calculated by the NOVA code with the poloidal harmonic range $m = 0 - 5$. The frequency of the mode is $\omega = 0.6\omega_A$. Fig. 4 shows the results of the comparison between the present FOW calculations and previous small orbit width expansion results [7]. Results from both codes agree well in the zero orbit width limit, i.e. for $z_h^{-1} \rightarrow 0$, but differ significantly when the orbit width becomes large. For example, for $z_h^{-1} = 2$ the radial width of trapped particle orbit is comparable with the mode localization width, and the fast ion growth rate is about 30% below the value obtained with the approximation of small orbit width expansion. However, for $z_h^{-1} > 2$, the orbit width becomes larger than the mode localization width and there is a significant difference in growth rate as compared with the small orbit width extension approach. In addition, the FLR further decreases the growth rate up to 50% at $z_h^{-1} \simeq 4$.

C. FOW and FLR effects on TAE Destabilization in TFTR

It turns out that FOW and FLR have different effects on core localized TAEs [16] and global TAEs. As an example we choose a global $n = 4$ mode with frequency $f = 253.4kHz$ for a TFTR equilibrium for the shot #73268 at $t = 3.41s$. The safety factors at the center and at the edge of the plasma are $q(r = 0) = 0.85$ and $q(r = a) = 5$, respectively. The central Alfvén velocity is $v_A = 8.36 \times 10^8 cm/s$. The alpha particles are taken as hot species and assumed to have a slowing down distribution function with a cutoff energy equal to their birth energy $\mathcal{E}_c = \mathcal{E}_{\alpha 0} = 3.52 MeV$. The eigenmode radial structure is shown in Fig. 5.

We have also analyzed a core localized TAE, which is considered to be responsible for the MHD plasma oscillations in the presence of alpha particles in TFTR DT experiments [11], where low amplitude magnetic perturbation were observed at $\delta B_\theta / B \simeq 10^{-5}$. We choose one of the TFTR DT shots: # 103101 at $2.92s$ where an $n = 4$ TAE was clearly seen for about $\sim 100ms$. The safety factor profile is quite flat at the center and has $q(r = 0) = 1.6$, and $q(r = a) = 5$. The central Alfvén velocity is $v_A = 1.19 \times 10^9 cm/s$. The TAE structure is shown in Fig. 6 and has a frequency $f = 214kHz$ which agrees with the observed frequency at $2.92s$. At this time the alpha particles born at the end of NBI are slowed down to the energy $\mathcal{E} \simeq 2.25MeV$, which we assume to be the cutoff energy in the slowing down distribution function.

Figures 7a and 7b show the FOW and FLR results for the $n = 4$ global and core localized TAE modes, respectively. Here the FOW scaling factor is introduced to reduce the α-particle orbit width to study the FOW effect without changing the equilibrium and other particle parameters. As shown in Fig. 7a, for the global mode, the FLR is stabilizing reducing the α growth by as much as a factor of 2.5 at full orbit width. On the other hand, the FOW is destabilizing because more particles from the central plasma region can reach the global TAE mode location. In the case of core localized TAE, we find that both FLR and FOW are stabilizing with up to a factor of 2 reduction in the growth rate due to FLR and a $\simeq 30\%$ reduction due to FOW effects. Note that FLR reduction occurs because $k_\perp \rho_\alpha \simeq 1$ for the parameter of the TFTR plasma, which gives $J_0^2(k_\perp \rho_\alpha) \simeq 1/2$.

IV. SUMMARY

A new version of NOVA-K has been developed. The improved code is capable of treating MHD modes perturbatively including full orbit width effects and finite Larmor radius effects. It was successfully benchmarked against the older versions of NOVA-K for the zero and small orbit width cases. We demonstrated that, in TFTR, the FOW can be either stabilizing in case of core localized TAE or destabilizing for the global TAE modes, depending on whether the orbit width effect can provides more particles in the region of mode location. The FLR is found to be always stabilizing. In future studies, the new NOVA-K code will be applied to study the stability of TAE and other MHD modes in devices such as spherical torus, where there is a concern of the confinement of super-Alfvenic ion population (such as NBI, ICRF ions) in the presence of collective instabilities.

ACKNOWLEDGMENT

This work was supported by US DoE contract DE-AC02-76-CHO-3073.

[1] C. Z. Cheng, L. Chen, and M. S. Chance, Ann. Phys. (N.Y.) **161**, 21 (1985).

[2] C. Z. Cheng, and M. S. Chance, Phys. Fluids **29**, 3695 (1986).

[3] K. L. Wong, R. J. Fonk, S. F. Paul, D. R. Roberts, E. D. Fredrickson, R. Nazikian, H. K. Park, M. Bell, L. Bretz, R. Budny, S. Cohen, G. W. Hammet, F. C. Jobes, D. M. Meade, S. S. Meadley, D. Mueller, Y. Nagayama, D. K. Owens, and E. J. Synakowski, Phys. Rev. Lett. **66**, 1874 (1991).

[4] W. W. Heidbrink, E. J. Strait, E. Doyle, and R. Snider, Nucl. Fusion **31**, 1635 (1991).

[5] D. J. Sigmar, C. T. Hsu, R. White, and Cheng C. Z., Phys. Fluids **B 4**, 1492 (1992).

[6] C. Z. Cheng, *Phys. Reports* **211** 1 (1994).

[7] Fu G. Y., Cheng C. Z., Wong K. L., *Phys. Fluids B* **5** 4040 (1994).

[8] F. Porcelli, R. Stankiewicz, W. Kerner, *Plasma Phys.* **1** 470 (1994).

[9] S. V. Putvinskii, in Reviews of Plasma Physics, Vol.18 (KADOMTSEV, B. B., Ed.), Consultants Bureau, New York (1986) 239.

[10] D. J. Grove and D. M. Meade, Nucl. Fusion **25**, 1167 (1985)

[11] R. Nazikian, G. Y. Fu, S. H. Batha, M. G. Bell, R. E. Bell, R. V. Budny, C. E. Bush, Z. Chang, Y. Chen, C. Z. Cheng, D. S. Darrow, P. C. Efthimion, E. D. Fredrickson, N. N. Gorelenkov, B. Leblanc, F. M. Levinton, R. Majeski,1 E. Mazzucato, S. S. Medley, H. K. Park, M. P. Petrov, D. A. Spong, J. D. Strachan, E. J. Synakowski, G. Taylor, S. Von Goeler, R. B. White, K. L. Wong, and S. J. Zweben, Phys. Rev. Letters **78**, 2976 (1997).

[12] R. V. Budny, Nucl. Fusion **34** 1247 (1994)

[13] A. I. Morozov and L. S. Solov'ev, in Reviews of Plasma Physics, Vol.2 (Acad. Leontovich, M.

A., Ed.), Consultants Bureau, New York (1966) 201.

[14] P. J. Catto, et al., *Plasma Phys.* **23** 639 (1981).

[15] N. N. Gorelenkov and C. Z. Cheng, Phys. Plasmas **2**, 1961 (1995).

[16] G. Y. Fu, Phys. Plasmas **2** 1029 (1995).

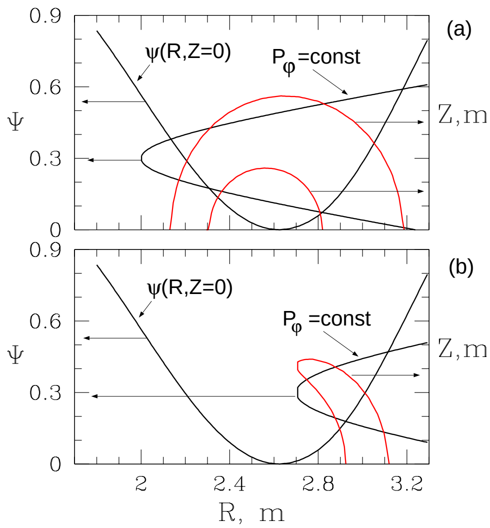

FIG. 1. Passing (a) and trapped (b) particle orbits represented in both (R,ψ) and (R,Z) planes for TFTR shot # 103101 at $2.92s$, when TAE was observed. The $\psi(R,Z=0)$ curve is the poloidal flux in the midplane.

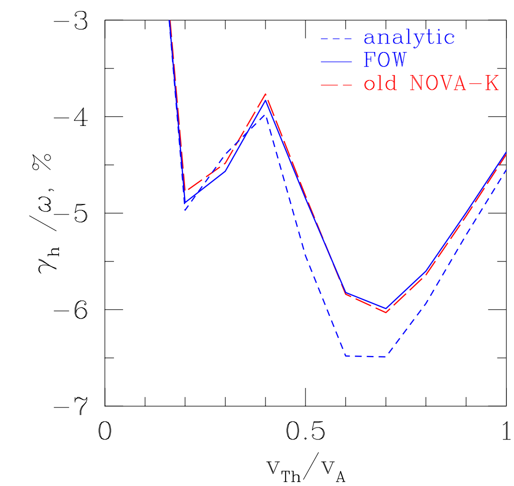

FIG. 2. Comparison of new FOW calculations of Landau damping on fast particles with old NOVA-K version and with "analytical" damping rates for $R_0/a = 10/3$.

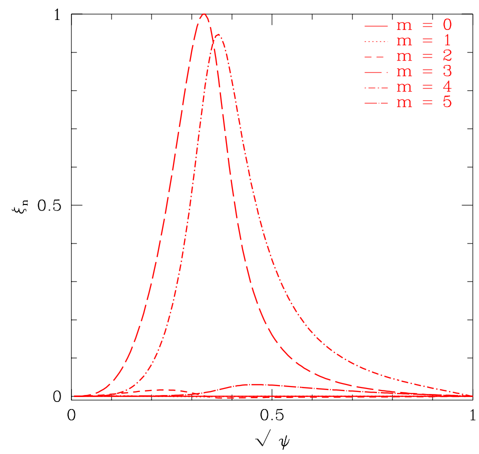

FIG. 3. The Fourier harmonics of the $n = 2$ TAE eigenfunction in the model equilibrium.

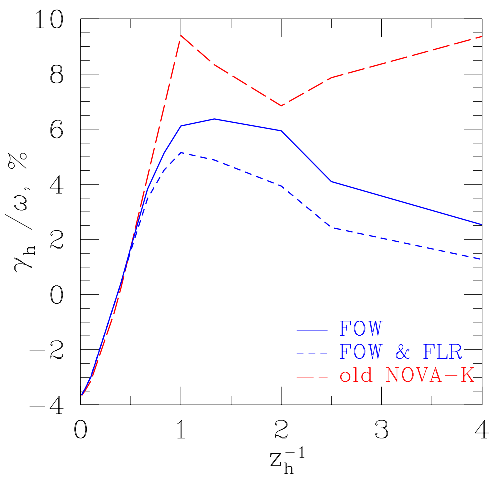

FIG. 4. Comparison between the new version of NOVA-K with full orbit width calculations and previous NOVA-K results employing small orbit width expansion.

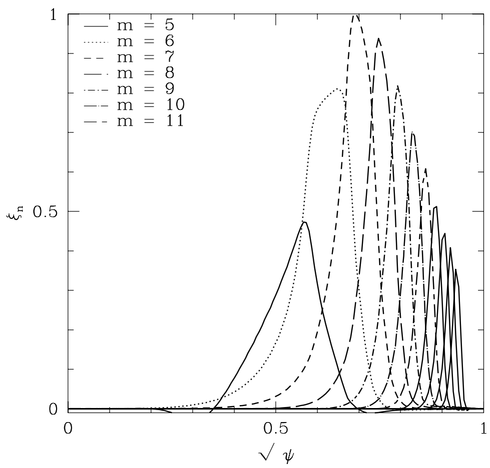

FIG. 5. Radial structure of poloidal harmonics of the radial displacement of $n = 4$ global TAE mode obtained by NOVA for TFTR shot # 73268 at 3.41s.

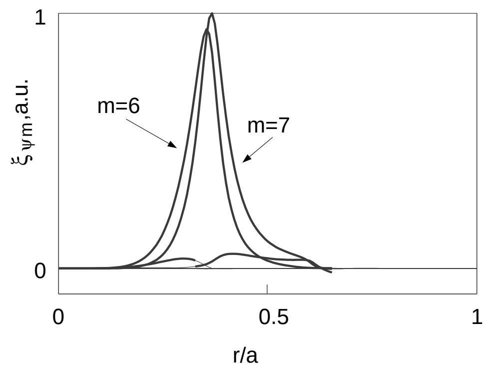

FIG. 6. Radial structure of poloidal harmonics of the radial displacement of $n = 4$ core localized TAE mode obtained by NOVA for TFTR shot # 103101 at $2.92s$.

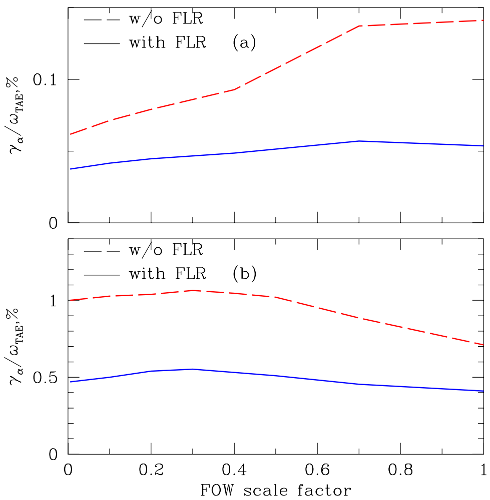

FIG. 7. Alpha particle driven TAE growth rate for (a) global TAE Fig.(5) in TFTR shot # 73268 at 3.41s; and (b) core localized TAE (Fig.6) in TFTR shot # 103101 at 2.92s.